Experimental Signature of Phonon-Mediated Spin Relaxation in a Two-Electron Quantum Dot

T. Meunier,[1] I. T. Vink,[1] L. H. Willems van Beveren,[1] K-J. Tielrooij,[1] R. Hanson,[1] F. H. L. Koppens,[1] H. P. Tranitz,[2]
W. Wegscheider,[2] L. P. Kouwenhoven,[1] and L. M. K. Vandersypen[1]

[1]*Kavli Institute of Nanoscience, Delft University of Technology, P.O. Box 5046, 2600 GA Delft, The Netherlands*
[2]*Institut für Angewandte und Experimentelle Physik, Universität Regensburg, Regensburg, Germany*
(Received 19 September 2006; published 22 March 2007)

We observe an experimental signature of the role of phonons in spin relaxation between triplet and singlet states in a two-electron quantum dot. Using both the external magnetic field and the electrostatic confinement potential, we change the singlet-triplet energy splitting from 1.3 meV to zero and observe that the spin relaxation time depends nonmonotonously on the energy splitting. A simple theoretical model is derived to capture the underlying physical mechanism. The present experiment confirms that spin-flip energy is dissipated in the phonon bath.

Relaxation properties of a quantum system are strongly affected by the reservoir where energy is dissipated [1]. Understanding which reservoir dominates dissipation can thus point at strategies for minimizing relaxation, and thereby improving coherent control of quantum systems. In this context, relaxation of electron spins embedded in nanostructures is of particular relevance, both for spintronic and spin-based quantum information processing devices [2]. For free electrons in a two dimensional electron gas (2DEG), spin relaxation times T_1 up to a few ns have been observed [3]. Here energy is easily given to the motion. In quantum dots, the discrete orbital energy level spectrum imposes other energy transfer mechanisms. Experiments showed that electron spins in quantum dots relax only after about one μs [4] near zero magnetic field, by direct flip-flops with the surrounding nuclear spins. Away from zero magnetic field, even longer spin relaxation times, 100 μs–100 ms, were observed [4–9]. Here, direct spin exchange with nuclei is suppressed and the phonon bath is expected to become the dominant reservoir in which spin-flip energy can be dissipated.

Direct spin relaxation by phonons is negligible [10], but phonons do couple to electron orbitals, and, through the spin-orbit interaction, can still couple to electron spins indirectly. Spin energy can thus be dissipated in the phonon bath [10–12]. Energy conservation requires that the phonon energy corresponds to the energy separation between the excited and the ground spin state. Changing the energy separation affects the efficiency of electron spin relaxation in two ways. First, since the phonon density of states increases with energy, the relaxation rate is expected to increase with energy as well. Furthermore, the electron-phonon interaction is highly dependent on the phonon wavelength in comparison to the dot size [13,14]. Specifically, we expect a suppression of relaxation for very large and for very small phonon wavelengths. The resulting maximum in the relaxation rate has never been observed so far [4–9], but would provide insight in the role

of the electron-phonon interaction in spin relaxation, as well as an understanding of the limitations on T_1.

Here, we study the spin relaxation time from triplet to singlet states for different energy separations in a single quantum dot containing two electrons. Singlet and triplet states have, respectively, two electrons in the lowest orbital and one electron each in the lowest and in the first excited orbital. In the experiment, the energy splitting $\Delta E_{S,T}$ between these two-electron spin states could be tuned from 0.9 meV to zero with a perpendicular magnetic field and from 0.8 to 1.3 meV by deforming the dot potential [15,16]. This energy range is an order of magnitude larger than in previous T_1 studies and it allows us to experimentally access the regime where the size of the dot versus the phonon wavelength is important.

All the experiments are performed in a dilution refrigerator with a quantum dot and a quantum point contact (QPC) defined in a 2DEG [see inset of Fig. 1(b)]. The conductance of the QPC is tuned to about e^2/h, making it very sensitive to the charge on the dot [17]. The sample is mounted with an angle $\phi = 68° \pm 5°$ between the normal to the 2DEG and the direction of the magnetic field B, where ϕ is derived from Shubnikov–de Haas oscillations. The electron temperature was measured to be 180 mK from the width of the Coulomb peaks. The lattice temperature was 50 mK.

We extract experimentally the energy splitting $\Delta E_{S,T}$ between the singlet and the triplet states as a function of both magnetic field B and the confinement potential using a pulse spectroscopy technique [18]. The dependence of $\Delta E_{S,T}$ on B is presented in Fig. 1(a). Up to 0.4 T, $\Delta E_{S,T}$ does not vary significantly with magnetic field which we relate to the elliptic nature of the dot at zero magnetic field [19]. For B larger than 0.4 T, $\Delta E_{S,T}$ decreases, to a good approximation, linearly with magnetic field. For energy separations below 100 μeV, the thermal broadening of the reservoir prevents us to measure $\Delta E_{S,T}$. From extrapolation of the data, we can determine the magnetic field
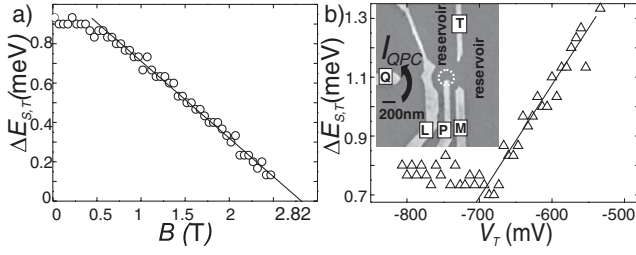
P H Y S I C A L   R E V I E W   L E T T E R S

FIG. 1. (a) Dependence of the energy splitting $\Delta E_{S,T}$ on magnetic field B. (b) Dependence of the energy splitting $\Delta E_{S,T}$ on the voltage V_T applied on gate T at $B = 0$. Inset: Scanning electronic micrograph showing the sample design. The 2DEG, located 90 nm below the surface of a GaAs/AlGaAs heterostructure, has an electron density of 1.3×10^{15} m^{-2}. By applying negative voltages to gates L, M, T, and Q we define a quantum dot (white dotted circle) and a QPC. Gate P is used to apply fast voltage pulses that rapidly change the electrochemical potentials of the dot. We tune the dot to the few-electron regime [27], and completely pinch off the tunnel barrier between gates L and T, so that it is only coupled to one electron reservoir at a time [18]. A voltage bias of 0.7 mV induces a current through the QPC, I_{QPC}, of about 30 nA. Tunneling of an electron on or off the dot gives steps in I_{QPC} of 300 pA [28,29]. The QPC measurement bandwidth is 100 kHz.

needed for singlet and triplet energy levels to cross: 2.82 ± 0.07 T.

We measure the relaxation time for varying $\Delta E_{S,T}$. To be able to measure T_1 close to the degeneracy point, we use a tunnel-rate selective readout procedure [8] (see Fig. 2). The measured spin relaxation time T_1 as a function of B is presented in Fig. 3. The shape of the T_1 dependence on magnetic field exhibits a striking nonmonotonous behavior. From 0.4 T to ~2 T, corresponding to a decrease in the energy splitting from 0.9 to 0.3 meV, the relaxation time first decreases, reaching a minimum of 180 μs. In between 2 T and the degeneracy point (2.82 T), T_1 increases whereas the energy splitting continues to decrease.

As a complementary study, we change $\Delta E_{S,T}$ in a different way by controlling the electrostatic potential of the dot via the voltage V_T applied to gate T and again look at T_1. The dependence of $\Delta E_{S,T}$ on V_T is presented in Fig. 1(b). With this second experimental knob, $\Delta E_{S,T}$ can be varied from 0.8 to 1.3 meV. We interpret the change in the observed energy splitting as a consequence of a change in the dot ellipticity. A more positive V_T implies a more circular dot and a larger energy splitting. We observe that T_1 further increases with $\Delta E_{S,T}$ as V_T is varied at $B = 0$ T (see the inset of Fig. 3). The maximum energy splitting reached at -530 mV, 1.3 meV, corresponds to a maximum of $T_1 = 2.3$ ms. With both experimental knobs, we observe that when $\Delta E_{S,T}$ is constant, T_1 is constant too (respectively, for $V_T < -650$ mV and $B < 0.4$ T). These observations clearly indicate that the most important parameter for the variation in the triplet-singlet relaxation time is their energy separation.
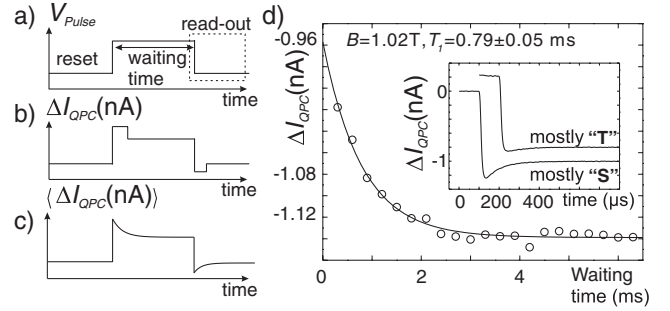

FIG. 2. (a) Voltage pulses applied to gate P for the relaxation measurement. The starting point is a dot with one electron in the ground state (initialization). During the pulse, the singlet and triplet electrochemical potentials are below the Fermi energy and a second electron tunnels into the dot. Because of the difference in tunnel rates [8], most likely a triplet state will be formed. We allow relaxation to occur during a waiting time that we vary. After the pulse, both electrochemical potentials are moved back above the Fermi energy and an electron tunnels out. This last step allows us to read out the spin state. (b) Schematic of the ΔI_{QPC} induced by the voltage pulse on gate P. If the state was singlet, a step from a slow tunneling event is added to the QPC response just after the readout pulse. If the state was triplet, the tunneling event is too fast to be observed. (c) After averaging over many single traces, a dip is observed and its amplitude is proportional to the probability of having singlet present in the dot. (d) Relaxation curve obtained for $B = 1.02$ T constructed by plotting the dip amplitude of the averaged traces at a predefined time after the readout pulse. The relaxation time, $T_1 = 0.79 \pm 0.05$ ms, is extracted from an exponential fit to the data (all the data are taken with a 100 kHz low-pass filter). Inset: curve resulting from the averaging over 500 individual traces for the longest waiting time (20 ms) and for the shortest waiting time (300 μs), offset by 100 μs and 0.2 nA for clarity.

The observed minimum in T_1 is precisely what one would expect for energy relaxation mediated by the electron-phonon interaction [14,20]. Indeed, the energy splitting $\Delta E_{S,T}$ determines the relevant acoustic phonon energy (acoustic phonons are the only available phonons for the explored energy range). At $B \sim 2$ T, $\Delta E_{S,T} \sim$ 0.3 meV, the associated half-wavelength, approximately 30 nm (the group velocity for acoustic phonons $c_s \sim$ 4000 m/s), is comparable to the expected size of the dot and therefore the coupling of the electrons in the dot to phonons is strongest. For energy separations smaller (larger) than 0.3 meV, the phonon wavelength is larger (smaller) than the size of the dot, the coupling to the orbitals becomes smaller and T_1 increases. The T_1 minimum at 0.3 meV directly points at energy dissipation in the phonon bath. Moreover, it is incompatible with dissipation in other possible reservoirs, such as photons, nuclear spins, and (virtual) electron exchange with the leads.

To get more insight in the role of the phonon wavelength, we present a simplified model of the energy relaxation process between triplet and singlet as a function of their energy splitting $\Delta E_{S,T}$. From Fermi's golden rule, the relaxation rate between the triplet and the singlet states
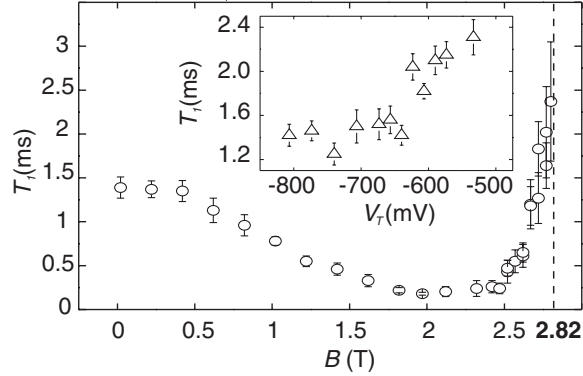
FIG. 3.   The spin relaxation time T_1 as a function of the magnetic field. The magnetic field where singlet and triplet states are degenerate is indicated by the dashed line. A minimum in T_1 is observed around 2.2 T. The error bars represent 70% confidence intervals. For energy separations close to degeneracy, the measurement sensitivity is reduced and the uncertainty in T_1 increases. Inset: dependence of the relaxation time T_1 on V_T at $B = 0$ T.

with energy separation $\Delta E_{S,T}$ is proportional to their coupling strength through electron-phonon interaction and to the phonon density of states at the energy $\Delta E_{S,T}$ [14,20]. To obtain a simple analytical expression, we assume that the only effect of the perpendicular magnetic field, the Coulomb interaction between electrons and the modification of the potential landscape is to change the energy splitting. Especially, their effects on the spatial distribution of the wave functions are neglected and we neglect the Zeeman energy. Furthermore, we restrict the state space of the analysis to $|T_-\rangle$, $|T_+\rangle$, $|T_0\rangle$, and $|S\rangle$ constructed from the lowest energy orbital and the first excited orbital (even though the contributions to triplet-singlet relaxation from higher orbitals can in fact be important [20]). In the notation $|T_-\rangle$, $|T_+\rangle$, $|T_0\rangle$, and $|S\rangle$, both the orbital part (assuming Fock-Darwin states) and the spin part are present. Finally, we also neglect higher order (e.g., two-phonon) processes, which are important at small magnetic field [21].

In contrast to the one electron case [10–12], the spin-orbit interaction admixes directly the first excited states $|T_\pm\rangle$ with the ground state $|S\rangle$. Because of the selection rules of the spin-orbit interaction, it does not affect $|T_0\rangle$ in lowest order [22]. As a consequence, the spin relaxation time of $|T_0\rangle$ can be much longer than $|T_\pm\rangle$ [23]. However, we do not observe any signature of a slowly relaxing component in the experiment. Since the spin-orbit coupling strength M_{SO} is small in comparison with $\Delta E_{S,T}$ (in the range accessed in the experiment), we can approximate the new eigenstates of the system as

$$|S'\rangle = |S\rangle - \frac{M_{SO}}{\Delta E_{S,T}}(|T_+\rangle + |T_-\rangle),$$

$$|T'_\pm\rangle = |T_\pm\rangle + \frac{M_{SO}}{\Delta E_{S,T}}|S\rangle.$$

In general, M_{SO} is dependent on the magnetic field [20,21], but to simplify the discussion, we neglect this dependence. Since the electron-phonon interaction preserves the spin, the coupling between $|T'_\pm\rangle$ and $|S'\rangle$ has the following form:

$$\langle T'_\pm|H_{e,p}|S'\rangle = \frac{M_{SO}}{\Delta E_{S,T}}(\langle S|H_{e,p}|S\rangle - \langle T_\pm|H_{e,p}|T_\pm\rangle),$$

where $H_{e,p} \sim e^{i\mathbf{q}\cdot\mathbf{r_1}} + e^{i\mathbf{q}\cdot\mathbf{r_2}}$ is the interaction Hamiltonian between electrons and phonons, $\mathbf{q}$ the phonon wave vector, and $\mathbf{r_i}$ the positions of the electrons. One can then interpret the coupling between $|T'_\pm\rangle$ and $|S'\rangle$ as the difference of the electron-phonon interaction strength for the corresponding unperturbed states $|T_\pm\rangle$ and $|S\rangle$. If the phonon wavelength is much larger than the dot size, the coupling to the phonons is the same for both states and the two terms will cancel. If the phonon wavelength is much shorter than the dot size, the coupling is small for each state separately.

To provide a quantitative comparison to the data, we need to model the electron-phonon interaction. Following [11,14], we assume bulklike 3D phonons. For the energy separations discussed in our experiment, only acoustic phonons are relevant. The Hamiltonian $H_{e,p}$ has then the following expression:

$$H_{e,p} = \sum_{j,\mathbf{q}} \frac{F_z(q_z)}{\sqrt{2\rho q c_j/\hbar}}(e^{iq_\| r_1} + e^{iq_\| r_2})(e\beta_{j,\mathbf{q}} - iq\Xi_{j,\mathbf{q}}),$$

where $(\mathbf{q}, j)$ denotes an acoustic phonon with wave vector $\mathbf{q} = (\mathbf{q}_\|, q_z)$, j the phonon branch index, and $\rho = 5300$ kg/m^3 is the density of lattice atoms. The factor $F_z(q_z)$ depends on the quantum well geometry and is assumed to be 1 in our model [14]. The speed of sound for longitudinal and transverse phonons are, respectively, $c_l = 4730$ m/s and $c_t = 3350$ m/s. We consider both piezoelectric and deformation potential types of electron-phonon interaction. In the considered crystal, the deformation potential interaction is nonzero only for longitudinal phonons (with a coupling strength $\Xi = 6.7$ eV). In contrast, all phonon polarizations j are important for piezoelectric coupling. The coupling strength depends on θ, defined as the angle between the wave vector and the growth axis, and varies for different polarizations as $e\beta_{j,\mathbf{q}} = A_j(\theta)e\beta$ where $e\beta = 1.4 \times 10^9$ eV/m [11,24]. Because of the different dependence on q for both mechanisms ($\sqrt{q}$ for deformation potential interaction, $1/\sqrt{q}$ for piezoelectric interaction), the piezoelectric (the deformation potential) coupling between electrons and phonons is dominant for energy separations below (above) 0.6 meV. From direct application of Fermi's golden rule, we derive the following analytical expression for the spin relaxation rate $1/T_1$:
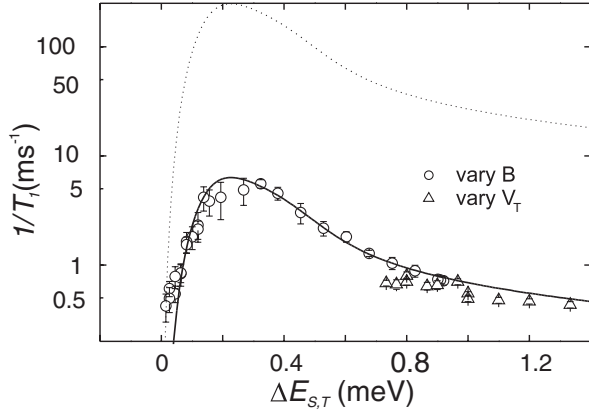
FIG. 4.   Relaxation rate as a function of the energy splitting $\Delta E_{S,T}$ deduced from the experimental data. The circles and the triangles correspond to the experiment where we vary, respectively, the magnetic field and the dot potential. The solid (dotted) line is the curve for $M_{SO} = 0.37$ μeV ($M_{SO} = 2.31$ μeV) obtained from the simplified model.

$$1/T_1 = \frac{M_{SO}^2}{32\pi\rho\hbar^3}\left(\frac{\Xi^2 a^4}{\lambda_{l,t}^5 c_l^4}\int_0^{\pi/2} d\theta\sin^5\theta e^{-(a^2\sin^2\theta)/(2\lambda_l^2)}\right.$$

$$+ \sum_{j=l,t}\frac{e^2\beta^2 a^4}{\lambda_j^3 c_j^4}$$

$$\left. \times \int_0^{\pi/2} d\theta|A_j(\theta)|^2\sin^5\theta e^{-(a^2\sin^2\theta)/(2\lambda_j^2)}\right),$$

where a is the dot radius (in our model a is independent of $\Delta E_{S,T}$ and is estimated to be 23 nm, from the measured single particle level spacing) and $\lambda_{l,t} = 2\pi\lambda_{l,t} = hc_{l,t}/\Delta E_{S,T}$ is the phonon wavelength. This simple model reproduces the most important feature in the measurements, which is that the coupling to the phonons vanishes for large and small energy separations and is strongest when the phonon wavelength matches the dot size (see Fig. 4).

The spin-orbit strength M_{SO} appears in the expression of $1/T_1$ only as a scaling factor. With a value $M_{SO} = 0.4$ μeV (corresponding to a spin-orbit length equal to $\hbar^2/2\alpha m^* M_{SO} \approx 50$ μm), the model reproduces the peak amplitude of the data quite well (Fig. 4, solid line). However, this value for M_{SO} is about 6 times smaller than the values reported in [9,25] (the dotted line in Fig. 4 corresponds to the relaxation rate using this value of M_{SO} in the model). The discrepancy could be the result of the exclusion of higher orbitals and the magnetic field dependence of M_{SO} in our model [20,21]. Again, we emphasize that both curves have a maximum corresponding to a phonon wavelength matching the dot size.

For single electron spin states, comparable variations of T_1 with the energy splitting are expected [10–12] although direct spin-orbit coupling between Zeeman sublevels of the same orbital is zero. To maximize the relaxation time of electron spin qubits, one needs then to choose an energy separation between the spin states such that the corre-

sponding phonon wavelength is different from the dot size. To complete our study of spin relaxation, it will be interesting to rotate the sample with respect to the magnetic field since the spin-orbit coupling strength depends on the angle between the crystallographic axis and the magnetic field [10,11,26].

[1] A. J. Leggett *et al.*, Rev. Mod. Phys. **59**, 1 (1987).
[2] *Semiconductor Spintronics and Quantum Computation*, edited by D. Awshalom, N. Samarth, and D. Loss (Springer-Verlag, Berlin, 2001).
[3] Y. Ohno *et al.*, Phys. Rev. Lett. **83**, 4196 (1999).
[4] A. C. Johnson *et al.*, Nature (London) **435**, 925 (2005).
[5] T. Fujisawa *et al.*, Nature (London) **419**, 278 (2002).
[6] J. M. Elzerman *et al.*, Nature (London) **430**, 431 (2004).
[7] M. Kroutvar *et al.*, Nature (London) **432**, 81 (2004).
[8] R. Hanson *et al.*, Phys. Rev. Lett. **94**, 196802 (2005).
[9] S. Amasha *et al.*, cond-mat/0607110.
[10] A. V. Khaetskii and Y. V. Nazarov, Phys. Rev. B **61**, 12 639 (2000).
[11] V. N. Golovach, A. V. Khaetskii, and D. Loss, Phys. Rev. Lett. **93**, 016601 (2004).
[12] J. L. Cheng, M. W. Wu, and C. Lü, Phys. Rev. B **69**, 115318 (2004); D. V. Bulaev and D. Loss, Phys. Rev. B **71**, 205324 (2005); P. Stano and J. Fabian, Phys. Rev. B **74**, 045320 (2006).
[13] T. Fujisawa *et al.*, Science **282**, 932 (1998).
[14] U. Bockelmann, Phys. Rev. B **50**, 17 271 (1994).
[15] L. P. Kouwenhoven, D. G. Austing, and S. Tarucha, Rep. Prog. Phys. **64**, 701 (2001).
[16] J. Kyriakidis *et al.*, Phys. Rev. B **66**, 035320 (2002).
[17] M. Field *et al.*, Phys. Rev. Lett. **70**, 1311 (1993).
[18] J. M. Elzerman *et al.*, Appl. Phys. Lett. **84**, 4617 (2004).
[19] D. G. Austing *et al.*, Phys. Rev. B **60**, 11 514 (1999).
[20] V. N. Golovach, A. V. Khaetskii, and D. Loss (to be published).
[21] P. San-Jose *et al.*, Phys. Rev. Lett. **97**, 076803 (2006).
[22] S. Dickmann and P. Hawrylak, JETP Lett. **77**, 30 (2003).
[23] S. Sasaki *et al.*, Phys. Rev. Lett. **95**, 056803 (2005).
[24] For longitudinal phonons, the piezoelectric constant $A_l(\theta) = 3\sqrt{2}/4\sin^2(\theta)\cos\theta$. For the two transverse polarizations, $A_{t1}(\theta) = \sqrt{2}/4\sin 2\theta$ and $A_{t2}(\theta) = \sqrt{2}/4(3\cos^2\theta - 1)\sin\theta$.
[25] D. M. Zumbuhl *et al.*, Phys. Rev. Lett. **89**, 276803 (2002).
[26] V. I. Fal'ko, B. L. Altshuler, and O. Tsyplyatyev, Phys. Rev. Lett. **95**, 076603 (2005).
[27] M. Ciorga *et al.*, Phys. Rev. B **61**, R16315 (2000).
[28] R. Schleser *et al.*, Appl. Phys. Lett. **85**, 2005 (2004).
[29] L. M. K. Vandersypen *et al.*, Appl. Phys. Lett. **85**, 4394 (2004).